Multipeaked probability distributions of recurrence times

Patrick Grete and Mario Markus*
Max-Planck-Institut für molekulare Physiologie, Postfach 500247, 44202 Dortmund, Germany
(Received 26 June 2006; revised manuscript received 4 September 2006; published 13 March 2007)

We determine probabilities of recurrence time into finite-sized, physically meaningful subsets of phase space. We consider three different autonomous chaotic systems: (i) scattering in a three-peaked potential, (ii) connected billiards, and (iii) Lorenz equations. We find multipeaked probability distributions, similar to the distributions found in (driven) stochastically resonant systems. In nondriven systems, such as ours, only monotonic decaying distributions (exponentials, stretched exponentials, power laws, and slight variations or combinations of these) have hitherto been reported. Discrete peaks in autonomous systems have as yet escaped attention in autonomous systems and correspond to specific trajectory subsets involving an integer number of loops.

DOI: 10.1103/PhysRevE.75.036207 PACS number(s): 05.45.Pq, 02.50.−r

I. INTRODUCTION

Hitherto investigated autonomous systems exhibit the following types of recurrence time distributions to sufficiently small regions of phase space: (i) exponential decay $P(t) \propto e^{-\alpha t}$ ([1–6] and references in [7]), (ii) power-law decay $P(t) \propto t^{-\beta}$ ([4,8–10] and references in [7]), (iii) strechted exponential decay $P(t) \propto e^{(-bt)^{\gamma}}$ [11–13], (iv) "wavy" decay in a log-log-plot [14,15], and (v) combinations of decays (i)–(iv) (e.g., [16]). In the context of ergodic theory, it has been shown that monotonic decay is expected as the size of the recurrence region tends to zero [17,18]. In contrast, we will consider in the present work recurrence to finite-sized subsets of phase space, paying special attention to short-time behavior.

Probabilities of times for the recurrence into finite-sized regions of phase space are of importance in many nonlinear systems: (i) earthquakes [8,19–21], (ii) solar flares [9], (iii) wind speeds [11], (iv) stock market indices [22], (v) atmospheric temperatures [12], and (vi) turbulence at the edge of a confined plasma [1]. Moreover, recurrence times to finite-sized regions are of interest to chaotic scattering phenomena, which have been studied in many areas of science (see [2,10,23–26]). In fact, the recurrence time to the domain outside the scattering region is equal to the residence time—i.e., the time delay [7,16,27] or the collisional time [28]—in the scattering region.

We will show that considering recurrences to finite-sized domains can have a drastic consequence: namely, the appearence of pronounced peaks in the recurrence time distribution. We demonstrate this here for simple, prototypical systems having very diverse features, suggesting that the peaks may be generic and relevant in some of the practically exciting systems cited in the preceding paragraphs, as well as in ergodic theory.

Multipeaked distributions have as yet only been reported for stochastically resonant systems. In such systems an external, periodical driving is required and the peaks occur at times related to that driving (see Sec. V). In contrast, the peaks in our (autonomous) systems occur according to intrinsic properties, which vary from system to system, as described below.

We will start investigating classical scattering in a Hamiltonian system which involves a three-peaked potential. For reinjection, the three peaks are surrounded by a circular potential wall (Sec. II). In Sec. III we investigate a simpler Hamiltonian system: namely, two connected billiards. Finally, in Sec. IV, we examine a dissipative system: namely, Lorenz equations.

II. REINJECTED CLASSICAL SCATTERING IN A THREE-PEAKED POTENTIAL

We consider a particle in a two-dimensional (2D) potential given by

$$V(x,y) = \sum_{n=1}^{3} h e^{-(\vec{x} - \vec{x}_n)^2/b} + a^4 (x^2 + y^2)^2. \tag{1}$$

The first term describes the peaks within which scattering takes place. The second term describes a circular potential wall, which surrounds the three peaks and causes reinjection into the scattering region. The maxima of the peaks occur at the $\vec{x}_n$, which are given by $(0, 1/\sqrt{3})$, $(-1/2, -1/2\sqrt{3})$, and $(1/2, -1/2\sqrt{3})$—i.e., at the vertices of an equilateral triangle. h is the height, b is the width of the peaks of the potential, and a defines the size of the reinjection wall. We set the particle mass equal to unity, $h=29.5$, $b=0.185$, $a=1$, and the total energy $E=15.92$. Injection is possible at $E > E_{crit} = 15.88$.

We define the boundary between the inner (scattering) and outer (reinjecting) regions as the curve defined by $dV/dr=0$, where $r=\sqrt{x^2+y^2}$ is the distance from the center of the equilateral triangle. This boundary is shown by a dashed curve in Figs. 2 and 3, below. The figures also show the saddle points (open circles) and the maxima (solid circles) of the potential.

The times that are physically interesting are those for the recurrence to the inner region (residence in the outer region) and those for the recurrence to the outer region (residence in the inner region). The probability distributions of these

*Electronic address: markus@mpi-dortmund.mpg.de

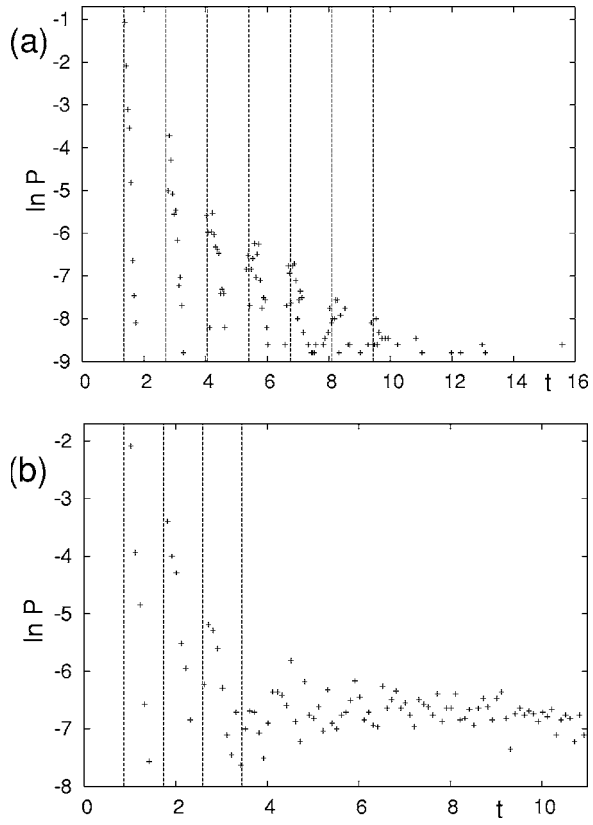

FIG. 1. Probability P of recurrence times to the inner region (a) and to the outer region (b) of a scattering system consisting of a three-peaked potential sorrounded by a reinjecting potential wall, as given by Eq. (1). (a), (b) The vertical, dashed lines indicate the theoretical evaluations using Eq. (2) as explained in the text.

times, obtained numerically by starting a single trajectory within the stochastic regime and evaluating 6000 recurrences, are shown in Fig. 1. The discrete peaks in Fig. 1 correspond to specific sets of trajectories, as exemplified in Figs. 2 and 3. The nth peak ($n=1,2,3,\ldots$, counting from left to right) in Fig. 1(a) corresponds to n loops in the outer

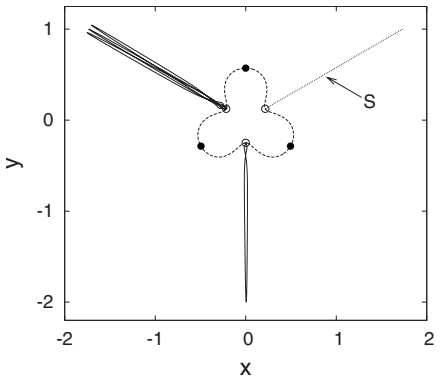

FIG. 2. Reinjecting trajectories outside the scattering region, consisting of one loop (bottom), which corresponds to the first peak in Fig. 1(a), and consisting of three loops (upper left), which correspond to the third peak in Fig. 1(a). Straight dotted line S: shortest trajectory. Open circles: saddles of the potential. Solid circles: potential maxima.

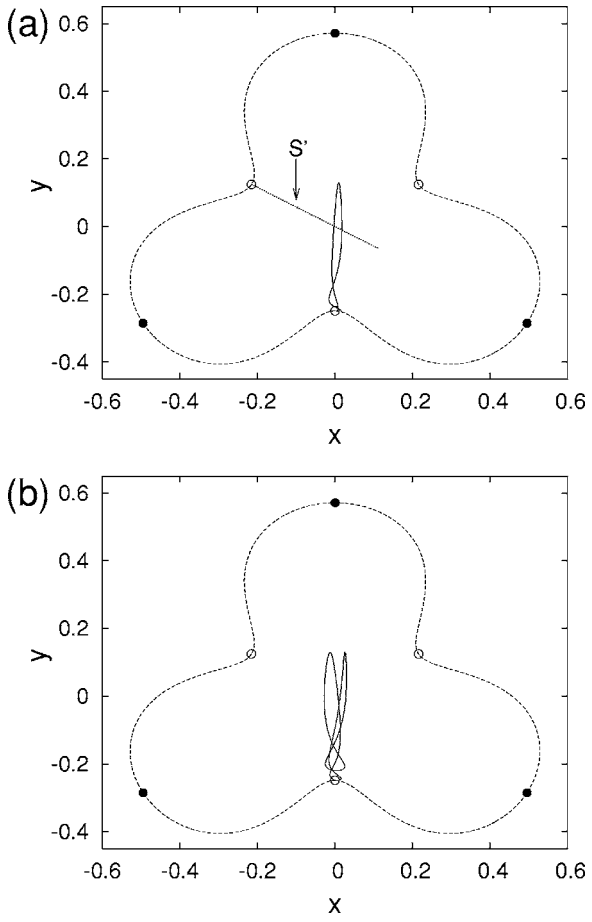

FIG. 3. Trajectories inside the scattering region, consisting of one loop (a), which corresponds to the first peak in Fig. 1(b), and consisting of two loops (b), which correspond to the second peak in Fig. 1(b). Straight dotted line S': shortest trajectory.

region, as illustrated in Fig. 2 for $n=1$ and $n=3$. The maximum of the first peak in Fig. 1(a) corresponds to the shortest loop, which follows a path such as the straight, dotted line S in Fig. 2. (There are two other equally short loops; they are obtained by rotating S around the origin by 60° and 120°.) The residence time T corresponding to these shortest loops can be calculated by considering $(dy/dt)^2/2 = E - V(0,y)$—i.e.,

$$T = 2\left|\int_{y_1}^{y_2} \frac{dy}{\sqrt{2(E - V(0,y))}}\right|, \tag{2}$$

where $dV/dr=0$ for $y=y_2$ and $E-V(0,y_1)=0$. Equation (2) yields $T_o=1.35$ for the outer shortest loop. In Fig. 1(a) we show this calculated value of T_o by the leftmost dashed vertical line. The other dashed vertical lines in this figure were drawn at integer multiples of T_o. One can see that these multiples are good approximations of the durations of the shortest trajectories with n loops. In fact, the particle moves back and forth closely to the shortest loop (straight, dotted line illustrated in Fig. 2); if it escapes after the nth approach to the boundary, then it corresponds to the left of the nth peak.

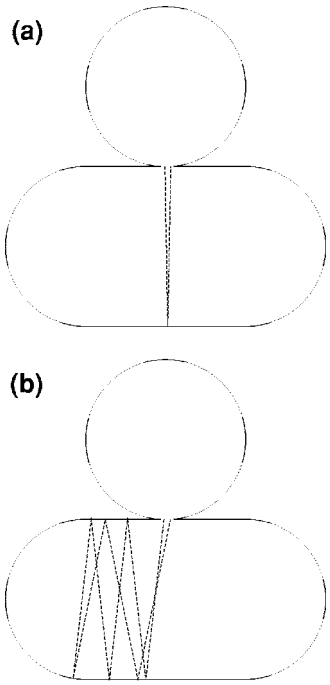

FIG. 4. Trajectories with one loop (a), corresponding to peak 1 in Fig. 5, and with four loops (b), corresponding peak 4 in Fig. 5.

The scenario is similar for the trajectories in the inner region. The nth peak (counting from left to right) in Fig. 1(b) corresponds to n loops in the inner region, as illustrated in Fig. 3(a) for $n=1$ and in Fig. 3(b) for $n=2$. The duration at the nth peak can be approximated by nT_i, where $T_i=0.86$ is obtained with Eq. (2) integrating along a straight loop, such as that indicated by the dotted line S' in Fig. 3(a). (S' is the shortest loop in the inner, scattering region; there are two other, equally short loops, which are obtained by rotating S' around the origin by 60° and 120°.) The resulting approximations nT_i are given by vertical, dashed lines in Fig. 1(b). As in Fig. 1(a), they are good approximations of the durations of the shortest trajectories with n loops. It is notewhorthy that for higher energies ($E \gtrsim 17$), we obtained single probability peaks between the peaks just described; the reason was that, in addition to moving in trajectories with n loops, the particle can escape near a saddle point that is not equal to the saddle point close to its entrance into the scattering region. If that happens after n loops, then this "sidewards" escape causes a peak between nT_i and $(n+1)T_i$.

In order to check the robustness of the results, not only with respect to changes in E, we also changed (for all investigated E) the scattering and reinjection geometry by using the following parameter sets (h,b,a) in Eq. (1): (40, 0.2, 1), (40, 0.2, 0.2), and (29.5, 0.2, 0.2). These parameter sets lead to multipeaked distributions similar to those in Fig. 1.

III. INTERMITTENCY IN CONNECTED BILLIARDS

Billiards connected through a hole are examples of configurations leading to intermittency in Hamiltonian systems [29]. We consider here a circle connected to a Bunimovich stadium, as shown in Fig. 4. We analyze numerically the recurrence times to the circle—i.e., the residence times in the stadium for a single trajectory—starting within the stochastic regime and analyzing 2.4×10^7 recurrences. The resulting probability distribution is shown in Fig. 5. As in the scattering system (Sec. II), the peaks can be associated with particular sets of "loops," which in the present system consist of straight segments, as illustrated for the first and fourth "loop" in Fig. 4.

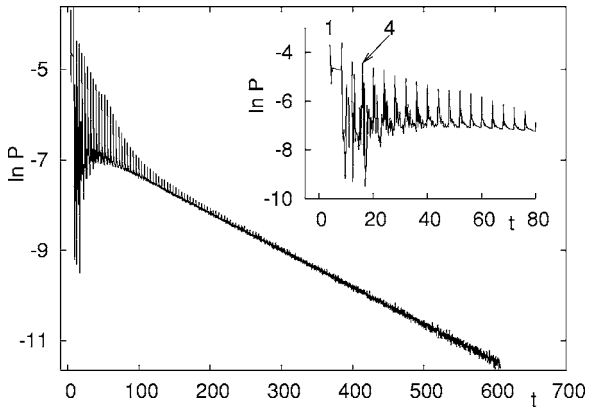

FIG. 5. Probability P of recurrence times to the circle at the top of Fig. 4 (residence time in the lower Bunimovich stadium).

We want to point out, that the peaks in Fig. 5 exist along the whole realm of the figure; they are superposed to the exponential tail and their amplitude decreases exponentially, so as to become unresolved for large t in the present figure. As a test for robustness, we changed the width of the stadium by a factor from 0.5 to 5.0 and obtained peaks similar to those in Fig. 5. Obviously a change of the height just changes the time between the peaks.

IV. LORENZ EQUATIONS

In contrast to the preceding sections, where we considered conservative systems, we consider here a dissipative system: namely, that described by the Lorenz equations [30]

$$\dot{x} = -\sigma x + \sigma y, \tag{3}$$

$$\dot{y} = rx - y - xz, \tag{4}$$

$$\dot{z} = -bz + xy. \tag{5}$$

We set $\sigma=10$, $r=28$, and $b=8/3$ and examine the recurrence to the scroll defined by $x>0$. In the original physical sense of these equations [30], the sign of x indicates the turning direction of convection rolls.

We integrated Eqs. (3)–(5) starting a single trajectory at $x=y=z=10^{-3}$ and waited 10^5 recurrences to allow the system to settle on the attractor; then, we evaluated 10^6 recurrences to get the probability distribution shown in Fig. 6. The nth peak ($n=1,2,\ldots$, counting from left to right) is associated with trajectories consisting of n loops, exemplified in Fig. 7 for $n=1$ and $n=5$.

The distance between the peaks can be estimated analytically, considering that the trajectory circles around an un-

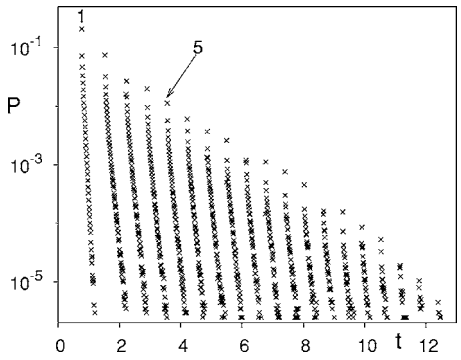

FIG. 6. Probability P of reccurrence times to positive x for the Lorenz equations (3)–(5).

stable fixed point F (see Fig. 7), because the Jacobi matrix has a complex eigenvalue λ there. Because the peaks correspond to complete loops around F, $T=2\pi/\mathrm{Im}(\lambda)\approx 0.62$ should be an approximation of the peaks's distance Δt. This is indeed the case for sufficiently large t ($t\gtrsim 3$); in fact, $\Delta t \approx 0.63$ (see Fig. 6). In contrast, the distance between the first two peaks is larger than T ($\Delta t\approx 0.76$) because these peaks correspond to rotations so far from F that deviations from the linear approximation leading to λ become noticeable.

As a test for robustness, we modified the condition $x<0$ to $x<a$ varying a within the interval $[-6,6]$. Also we modified r, which is proportional to the temperature difference in the original physical sense, to 40. Under any of these changes we optained peaks similar to those shown in Fig. 6. This robustness is explainable by the fact that the performed changes do not affect the cycling around the fixed point F, which causes the peaks.

V. DISCUSSION

Multipeaked distributions have as yet (except for stochastically resonant systems; see below) not been reported. The reasons are (i) only recurrences to small regions were considered (e.g., to small circles for Lorenz equations [3]), (ii) short times were not investigated [16] or not sufficiently resolved, and (iii) the appropiate method was not implemented; this is the case in the experimental study of circuits in [31], where the question of residence times in scrolls of attractors was explicitely posed, but only a Fourier analysis, which does not reveal the peaks, was performed.

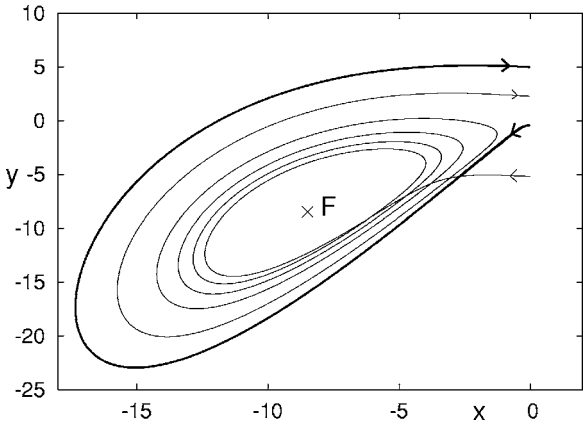

FIG. 7. Trajectories (projected on the x-y plane) with one loop (fat curve), corresponding to peak 1 in Fig. 6, and with five loops (thin curve), corresponding to peak 5 in Fig. 6. F: unstable fixed point.

We have shown here that multipeaked distributions of recurrence time are obtained for a variety of systems. Each peak corresponds to a subset of a chaotic trajectory, consisting of segments with a particular number of loops. There exist cases for which the peak maxima decay exponentially (Fig. 5 within some time intervals and Fig. 6), which is explained as follows. The probability of nonrecurrence after the n loops is $(1-p)^n$, where p is the probability of recurrence after one loop. The probability P of recurrence right after n loops thus is $p(1-p)^n$. Considering $n\propto t$ and defining $a=1/(1-p)>1$, we obtain $P\propto a^{-t}$.

Note that the orbits defining the peaks are neither periodic nor quasiperiodic. In fact, we found that small perturbations of n-looped orbits lead to loops with a different value of n. This value is the common property of the orbits determining a given peak. The duration of these orbits is not defined by single numbers, as in periodic or quasiperiodic orbits, but varies continuosly within the intervals between local peak maxima (see Figs. 1, 5, and 6).

In addition to the exponential decay of the peak maxima, we also obtained in some cases (see Figs. 1 and 6) an exponential (or nearly exponential) decay of each peak. This can be explained by the fluctuations around each n-fold loop and by assuming that these fluctuations follow the exponential decay generally observed for chaotic systems. These fluctuations entail recurrence times that are larger than at the peak maxima. In contrast to our exponentially decaying peaks, those peaks due to stochastic resonance are always bell shaped [17,18,32–36]; i.e., fluctuations can both increase or decrease the recurrence times, as compared to those at the maxima.

Stochastically resonant systems [17,18,32–36] are the only systems for which, to our knowledge, multipeak time distributions have hitherto been reported. In such systems an external signal is amplified with the help of noise [18,32,33,35] or of intrinsic chaotic fluctuations that play the role of an "effective" noise [17,34,36]. As explained in [33,32], the peaks then occur at times equal to nT_0 or $(2n-1)T_0$ ($n=1,2,3,\ldots$; T_0: period of the external signal). In contrast, the systems described here are not externally driven; thus, peak formation is described by intrinsic properties of the system.

Except for the case of the Lorenz equations (Sec. IV), we obtained asymptotic approaches to an exponential decay of $P(t)$ for large t. This is illustrated in Fig. 5 for the billiard system. In the case of the scattering system (Sec. II) we found that peaks are replaced by an exponential decay of P for large t if we extend the time interval considerably beyond that of Fig. 1. Time is then sufficiently large for chaos to disrupt n-looped trajectories and the situation becomes comparable to that reported for many cases in the literature (cited in Sec. I).

Multipeaked reccurrence time distributions, as those exhibited in this work, seem evident at first sight, in spite of

numerous counterexamples with no peaks, as that of other systems found in the literature (see, e.g., [1–3,5–16]). But there is no *a priori* reason to assume that a considerable number of peaks can occur before chaos destroys the n loops, rendering a monotonic decay of $P(t)$. Moreover, peaks may never be destroyed, as is the case for the Lorenz equations. Both in short-time or in indefinite phenomena, it is remarkable that abrupt changes of $P(t)$, owing to transitions from n to $n+1$ loops, "quantize" the system in a way that as yet has escaped attention.

We have shown that multipeaked distributions exist in highly dissimilar systems: conservative ordinary differential equations (ODE's), billiards, and dissipative ODE's. The diversity of these systems, as well as their in other aspects generic properties, suggests that our results are generic too. If there exist conditions for which this is true and if, in future work, multipeaked distributions were found in real climatic, tectonic, or other risky systems, then the occurrence of pronounced minima and maxima of probabilities would be of obvious importance.

ACKNOWLEDGMENT

We thank Malte Schmick for valuable discussions.

[1] M. Baptista, I. Caldas, M. Heller, A. Ferreira, R. Bengtson, and J. Stöckel, Phys. Plasmas **8**, 4455 (2001).
[2] P. Boyd and S. McMillan, Chaos **3**, 507 (1993).
[3] J. B. Gao, Phys. Rev. Lett. **83**, 3178 (1999).
[4] R. Bowen, Am. J. Math. **94**, 413 (1972).
[5] G. M. Zaslavsky and M. K. Tippett, Phys. Rev. Lett. **67**, 3251 (1991).
[6] M. Franaszek and E. Simiu, Phys. Lett. A **205**, 137 (1995).
[7] Y.-C. Lai, Phys. Rev. E **60**, R6283 (1999).
[8] X. Yang, S. Du, and J. Ma, Phys. Rev. Lett. **92**, 228501 (2004).
[9] G. Boffetta, V. Carbone, P. Giuliani, P. Veltri, and A. Vulpiani, Phys. Rev. Lett. **83**, 4662 (1999).
[10] E. Ziemniak, C. Jung, and T. Tél, Physica D **76**, 123 (1994).
[11] M. Santhanam and H. Kantz, Physica A **345**, 713 (2005).
[12] A. Bunde, J. F. Eichner, J. W. Kantelhardt, and S. Havlin, Phys. Rev. Lett. **94**, 048701 (2005).
[13] E. G. Altmann and H. Kantz, Phys. Rev. E **71**, 056106 (2005).
[14] E. G. Altmann, A. E. Motter, and H. Kantz, Phys. Rev. E **73**, 026207 (2006).
[15] M. Weiss, L. Hufnagel, and R. Ketzmerick, Phys. Rev. E **67**, 046209 (2003).
[16] A. E. Motter and Y.-C. Lai, Phys. Rev. E **65**, 015205(R) (2001).
[17] G. Nicolis, C. Nicolis, and D. McKernan, J. Stat. Phys. **70**, 125 (1993).
[18] V. Anishchenko, A. Neiman, and M. Safanova, J. Stat. Phys. **70**, 183 (1993).
[19] N. Scafetta and B. J. West, Phys. Rev. Lett. **92**, 138501 (2004).
[20] A. Corral, Phys. Rev. Lett. **92**, 108501 (2004).
[21] P. Bak, K. Christensen, L. Danon, and T. Scanlon, Phys. Rev. Lett. **88**, 178501 (2002).
[22] M. Baptista and I. Caldas, Physica A **312**, 539 (2002).
[23] D. Noid, S. Gray, and S. Rice, J. Chem. Phys. **84**, 2649 (1986).
[24] R. Blümel, Chaos **3**, 683 (1993).
[25] A. Péntek, T. Tél, and Z. Toroczkai, J. Phys. A **28**, 2191 (1995).
[26] C. Marcus, R. Westervelt, P. Hopkins, and A. Gossard, Chaos **3**, 643 (1993).
[27] S. Bleher, C. Grebogi, and E. Ott, Physica D **46**, 87 (1990).
[28] Y. Gu and J. M. Yuan, Phys. Rev. A **47**, R2442 (1993).
[29] M. Markus and M. Schmick, Physica A **328**, 335 (2003).
[30] E. Lorenz, J. Atmos. Sci. **20**, 130 (1963).
[31] P. Etchegoin, Physica A **97**, 97 (2001).
[32] A. Longtin, A. Bulsara, and F. Moss, Phys. Rev. Lett. **67**, 656 (1991).
[33] T. Zhou and F. Moss, Phys. Rev. A **41**, 4255 (1990).
[34] K. Arai, S. Mizutani, and K. Yoshimura, Phys. Rev. E **69**, 026203 (2004).
[35] M. H. Choi, R. F. Fox, and P. Jung, Phys. Rev. E **57**, 6335 (1998).
[36] K. Arai, K. Yoshimura, and S. Mizutani, Phys. Rev. E **65**, 015202(R) (2001).